

Geophysical Research Letters



RESEARCH LETTER

10.1029/2020GL091412

The authors Sentia Goursaud and Max Holloway are the joint first authors of the manuscript.

Key Points:

- The relationship of $\delta^{18}\text{O}$ against elevation at 128 kyr is not uniform across Antarctica
- The effect of the elevation can be isolated from that due to sea ice change
- Ice core results appear to unequivocally exclude the loss of the Wilkes Basin at around 128 kyr

Supporting Information:

- Supporting Information S1

Correspondence to:

M. Holloway,
Max.Holloway@sams.ac.uk

Citation:

Goursaud, S., Holloway, M., Sime, L., Wolff, E., Valdes, P., Steig, E. J., & Pauling, A. (2021). Antarctic ice sheet elevation impacts on water isotope records during the Last Interglacial. *Geophysical Research Letters*, 48, e2020GL091412. <https://doi.org/10.1029/2020GL091412>

Received 30 OCT 2020

Accepted 14 DEC 2020

Antarctic Ice Sheet Elevation Impacts on Water Isotope Records During the Last Interglacial

Sentia Goursaud¹ , Max Holloway² , Louise Sime³ , Eric Wolff¹ , Paul Valdes⁴ , Eric J. Steig⁵ , and Andrew Pauling⁵ 

¹Department of Earth Sciences, University of Cambridge, Cambridge, UK, ²Scottish Association for Marine Science, Oban, UK, ³Ice Dynamics and Paleoclimate, British Antarctic Survey, Cambridge, UK, ⁴School of Geographical Science, University of Bristol, Bristol, UK, ⁵Department of Atmospheric Sciences, University of Washington, Seattle, WA, USA

Abstract Changes of the topography of the Antarctic Ice Sheet (AIS) can complicate the interpretation of ice core water stable isotope measurements in terms of temperature. Here, we use a set of idealized AIS elevation change scenarios to investigate this for the warm Last Interglacial (LIG). We show that LIG $\delta^{18}\text{O}$ against elevation relationships is not uniform across Antarctica and that the LIG response to elevation is lower than the preindustrial response. The effect of LIG elevation-induced sea ice changes on $\delta^{18}\text{O}$ is small, allowing us to isolate the effect of elevation change alone. Our results help to define the effect of AIS changes on the LIG $\delta^{18}\text{O}$ signals and should be invaluable to those seeking to use AIS ice core measurements for these purposes. Especially, our simulations strengthen the conclusion that ice core measurements from the Talos Dome core exclude the loss of the Wilkes Basin at around 128 kyr.

Plain Language Summary The Last Interglacial (LIG) period (116,000–130,000 years ago) was globally $\sim 0.8^\circ\text{C}$ warmer than today at its peak, with substantially more warming at the poles. It is a valuable analog for future global temperature rise, especially for understanding rates and sources of polar ice melt and subsequent global sea level rise. Records of water stable isotopes from Antarctic ice cores have been crucial for understanding past polar temperature during the LIG. However, we currently lack a framework for estimating how changes in the ice sheet elevation, alongside sea ice feedbacks, affect these water stable isotopes. To address this, we examine the effect of the Antarctic Ice Sheet (AIS) elevation on water stable isotopes, using an ensemble of climate simulations where we vary the AIS elevation. We observe that (i) water stable isotope values lower with increasing AIS elevation following linear relationships and (ii) the effect of sea ice induced by AIS elevation is small so the effect of AIS elevation can be isolated. Finally, this study provides appropriate elevation-water stable isotope gradients for the reconstruction of the AIS topography using ice cores.

1. Introduction

The size and configuration of the Antarctic Ice Sheet (AIS) varies in response to mass balance (Scambos et al., 2017) and ice dynamics. Variations in the rate of accumulation are important across the continent (Ritz et al., 2001; Steig et al., 2013). Current West Antarctic Ice Sheet (WAIS) changes are driven by increasing melt, calving rates, and associated ice flow changes. These processes are sensitive to ocean temperature, alongside ocean and atmospheric circulation changes (Adusumilli et al., 2020; DeConto & Pollard, 2016; Pollard & DeConto, 2009; Scambos et al., 2017).

Geological data indicate that the WAIS expanded during the Last Glacial Maximum (LGM, approximately 21 kyears BP [ka]) (Bentley et al., 2014; Conway et al., 1999) and likely reduced during warmer interglacials (DeConto & Pollard, 2016; Dutton et al., 2015; Kopp et al., 2009, 2013; McKay et al., 2012; Scherer et al., 1998; Steig et al., 2015). It is less clear if the East AIS (EAIS) also reduced or expanded during interglacials (Sutter et al., 2020; Wilson et al., 2018). Last Interglacial (LIG) changes in insolation are also known to directly impact polar sea ice extent (Guarino et al., 2020; Kageyama et al., 2020).

It has been difficult to explain the LIG peak in $\delta^{18}\text{O}$ at 128 kyr in Antarctic ice core data (Sime et al., 2009). Holloway et al. (2016) provided a potential explanation for the observed signal, but we still lack understanding of how elevation, insolation, and sea ice jointly affect the water isotope signal. Since insolation and sea ice, in addition to AIS change, affect the isotopic signal in ice cores (Holloway et al., 2016, 2017;

© 2020. The Authors.

This is an open access article under the terms of the Creative Commons Attribution License, which permits use, distribution and reproduction in any medium, provided the original work is properly cited.

Malmierca-Vallet et al., 2018), it is necessary to understand how temperature, atmospheric circulation, spatially variable lapse rates, and sea ice feedbacks can all affect the recorded accumulation and isotopic signals when attempting to use these data to help us to deduce past AIS changes.

Werner et al. (2018) and Sutter et al. (2020) explored the use of $\delta^{18}\text{O}$ (and temperature) versus elevation relationships to help to evaluate possible AIS reconstructions. Werner et al. (2018) focused on the LGM using the isotope-enabled atmospheric general circulation model ECHAM5-wiso to produce a set of LGM simulations with different AIS reconstructions used in the framework of the Paleoclimate Modeling Inter-comparison Project (Otto-Bliesner et al., 2017). A model-data (ice core) $\delta^{18}\text{O}$ comparison allowed insight into the most likely LGM AIS configuration. More recently, Sutter et al. (2020) derived the most probable Wilkes configuration for the LIG by comparing $\delta^{18}\text{O}$ anomalies from the Talos Dome Ice Core with a suite of ice sheet model simulations using the Parallel Ice Sheet Model (Golledge et al., 2015). Sutter et al. (2016) inferred the LIG $\delta^{18}\text{O}$ signal for each of their model configurations using the present-day surface air temperature (SAT) versus elevation relationship from Frezzotti et al. (2007) to obtain temperature, and then to apply the SAT versus temperature derived from Werner et al. (2018). More generally, obtaining quantified information on LIG AIS loss from ice core measurements is still needed for the LIG community (Sime et al., 2019). The LIG AIS loss scenario is directly relevant to calculating future AIS loss probabilities (e.g., DeConto & Pollard, 2016; Edwards et al., 2019).

Here, we investigate the stable water isotope ($\delta^{18}\text{O}$) response to changes in AIS elevation at 128 kyr, using an ensemble of isotope-enabled climate model experiments from the HadCM3 model. We describe the patterns of SAT, precipitation, and $\delta^{18}\text{O}$ in response to elevation changes and compare isotope–elevation relationships at the continental scale as well as at the location of ice cores spanning the LIG. Finally, we briefly discuss how our results might be used to help to interpret LIG isotope signatures.

2. Materials and Methods

The isotopic response to idealized changes in AIS elevation is simulated using the isotope-enabled coupled ocean–atmosphere–sea ice General Circulation Model, HadCM3 (Tindall et al., 2009). Fractional isotopic content is expressed for oxygen-18 using standard $\delta^{18}\text{O}$ notation (Supporting information Text S1). Two control simulations were used: a preindustrial (PI) simulation, and a 128 ka simulation centered on the LIG Antarctic isotope maximum using a modern day AIS configuration (Holloway et al., 2016). Then, a suite of eight idealized AIS elevation change simulations were performed also including 128 ka orbital and greenhouse-gas forcing. Each elevation change experiment includes a simple scaling of the AIS to isolate the impact of ice sheet elevation on temperature, precipitation, and $\delta^{18}\text{O}$. The change in elevation across the AIS is scaled relative to the prescribed change at the EPICA Dome C (EDC) ice core site using a scaling coefficient β , where

$$\beta = \frac{Z_{EDC}}{(Z_{EDC} + \Delta z)}, \quad (1)$$

and Z_{EDC} is the EDC ice core site elevation in the modern day AIS configuration, Δz is the prescribed elevation change at EDC, which extends to $\pm 1,000$ m. Elevations across the Antarctic continent are then increased or decreased proportional to β :

$$Z'_A = Z_A / \beta \quad (2)$$

where Z_A is the two-dimensional array of modern AIS elevations and Z'_A is a new array of altered AIS elevations. Since this approach maintains the modern shape of the AIS, it reduces the influence of changing ice sheet configuration on circulation and climate and helps in isolating the effect of elevation changes alone. Experiments are performed with Δz equal to (\pm) 100, 200, 500, and 1,000 m (Supporting information Table S1). Each of the above elevation change scenarios is integrated for a total of 500 years to ensure that surface and middepth climate fields are sufficiently spun up with the imposed elevation changes. The last 50 years of each simulation are analyzed. We also include a simulation with the WAIS reduced to a uniform elevation of 200 m and remains ice covered, as published in Holloway et al. (2016), and following the approach of Holden et al. (2010).

LIG maximum values of +2–4‰ above PI in $\delta^{18}\text{O}$ are recorded in East Antarctic ice cores. We consider our elevation scenarios in the context of these LIG $\delta^{18}\text{O}$ published ice core records from East Antarctica (Masson-Delmotte et al., 2011): Vostok (Petit et al., 1999), Dome Fuji (DF, Kawamura et al., 2007), EDC (Jouzel et al., 2007), EPICA Dronning Maud Land (EDML, EPICA Community Members, 2006), Talos Dome Ice Core (TALDICE, Stenni et al., 2011), and Taylor Dome (Steig et al., 2000), as well as unpublished or planned LIG $\delta^{18}\text{O}$ ice core records from West Antarctica: West Antarctica Ice Sheet Divide, Hercules Dome, and Skytrain.

For all our statistical analyses, averages are given with their associated standard deviation (average \pm standard deviation). Linear relationships are considered significant when the p -value is lower than 0.05 (Supporting information Text S2).

3. Results

3.1. Changes in Antarctic SAT and Precipitation

The LIG forcing, with no AIS elevation change, induces a mean annual Antarctic warming of $0.9 \pm 0.6^\circ\text{C}$ compared to PI (Supporting information Table S2) and precipitation increases of 0.6 ± 1.3 mm/month. Changes are larger in the coastal regions and show wider regional differences: for example, precipitation increases on the coast of the Bellingshausen Sea but decreases on the coast of the Amundsen Sea (cf., Otto-Bliesner et al., 2020).

Increases in the elevation of AIS act to decrease SATs (Mechoso, 1980, 1981; Parish et al., 1994; Singh et al., 2016). The mean Antarctic SAT change is $+4.7 \pm 4.6^\circ\text{C}$ higher for the DC – 1 km experiment and $-4.4 \pm 4.2^\circ\text{C}$ for the DC + 1 km experiment, compared to the LIG control simulation (Figure 1).

Changes in precipitation with the elevation tend to follow SAT changes, that is, it decreases as the elevation of AIS is increased. Mean Antarctic precipitation anomalies compared to the LIG control simulation are 3.0 ± 4.7 mm/month for the DC – 1 km experiment and -2.4 ± 4.2 mm/month for the DC + 1 km experiment. The largest changes in precipitation occur along coasts facing the Indian Ocean, the Weddell Sea, and along the Ronne Ice Shelf, where the orographic slopes are the steepest (Supporting information Figure S1; Krinner & Genthon, 1999). Deviations from the SAT–precipitation relationships are also the largest in coastal areas (Figure 1). In particular, the Eastern part of the Peninsula and the WAIS coast display opposite elevation–precipitation relationships compared to the rest of the AIS. This may be due to changes in the localized Peninsula foehn-related drying and/or heat fluxes associated with a more stationary Amundsen Sea low when AIS topography is higher (Krinner & Genthon, 1999). These factors are liable to cause complications when interpreting accumulation change data from coastal and Peninsula ice cores during AIS changes (e.g., Medley & Thomas, 2019).

3.2. Antarctic Ice Core $\delta^{18}\text{O}$ Anomalies

Mean Antarctic $\delta^{18}\text{O}$ increases during the LIG by $0.6 \pm 0.8\text{‰}$ compared to PI. At the continental scale, when changing the entire AIS elevation, $\delta^{18}\text{O}$ changes closely follow both SAT and elevation (Figures 1 and 2). This result is consistent with Holloway et al. (2016) and Steig et al. (2015), who report strong positive anomalies over the WAIS when WAIS elevations are reduced to 200 m (“Flat WAIS” experiment hereafter). Our results indicate that $\delta^{18}\text{O}$ anomalies against PI are stronger when the elevation is decreased than when the elevation is increased, a feature also observed for SAT. For the DC – 1 km simulation, mean Antarctic $\delta^{18}\text{O}$ changes is $+6.5 \pm 2.9\text{‰}$, compared to the PI simulation and $-2.3 \pm 2.4\text{‰}$ for the DC + 1 km simulation. However, there are heterogeneous patterns in $\delta^{18}\text{O}$ anomalies—mainly in East Antarctica—in response to our idealized and linear elevation changes.

Figure 2 (and Supporting information Table S3) includes the $\delta^{18}\text{O}$ changes at existing and planned ice core drilling sites. Since these are idealized topographies, and there are other influences on $\delta^{18}\text{O}$, it is not surprising that none of the simulated elevation changes provide a match to the PI to LIG $\delta^{18}\text{O}$ differences observed in ice cores (Supporting information Table S4). The results of Holloway et al. (2016) show that a reduction

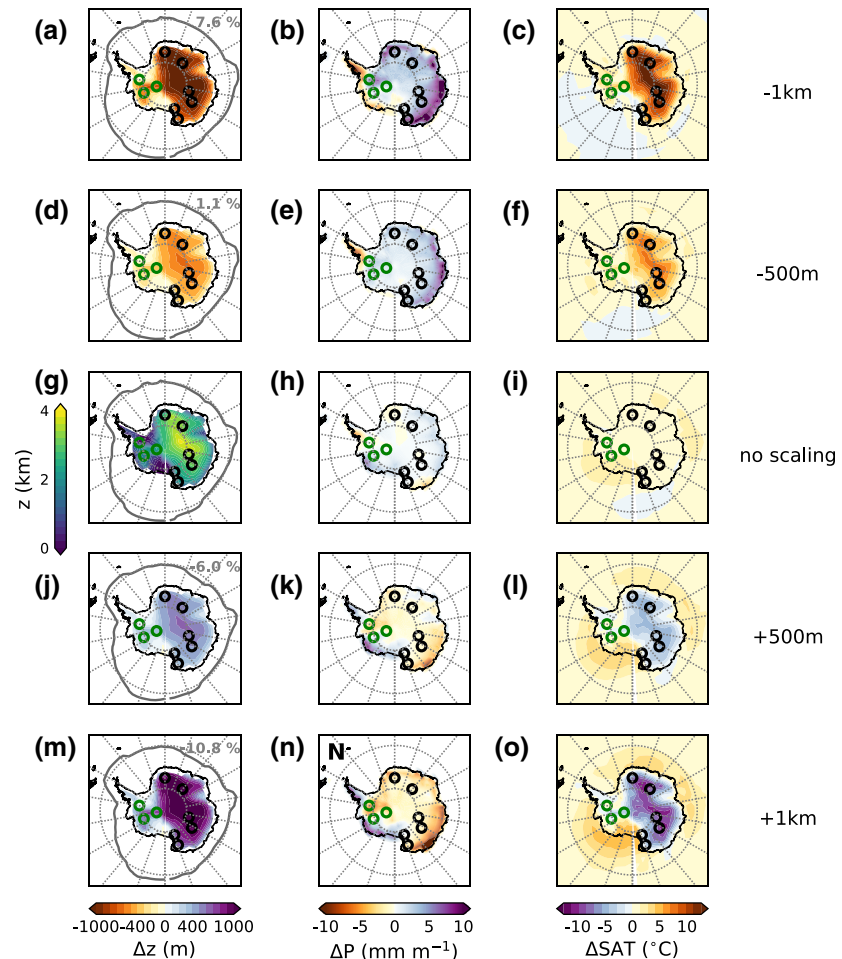


Figure 1. Patterns of idealized Antarctic Ice Sheet simulations. Map of Antarctic elevation change in response to elevation scaling of -1 km (first row), -500 m (second row), no scaling (third row), $+500$ m (fourth), and $+1$ km (last row), relative to the height at EDC. (g) The orography of the reference Antarctic configuration (“Z,” in km). The different panels (with the exception of (g)) display anomalies relative to a preindustrial control experiment using the reference Antarctic configuration, of (i) the orography (“ Δz ,” in m, first column) with the September sea ice extent ($\geq 15\%$, gray contours), (ii) precipitation (“ ΔP ,” in mm/month, second column), and (iii) the surface air temperature (“ ΔSAT ,” in $^{\circ}C$, third column). September sea ice anomalies are given in the top right of the figures giving the orography and the September sea ice extent. Ice core locations with available data are indicated by black points, whereas ice core locations with no available data are indicated by green points. EDC, EPICA Dome C.

in winter sea ice area of $65 \pm 7\%$ provides a closer match to the ice core data than any of the idealized AIS elevation change simulations presented here; it is thus of interest to understand how changes in ice sheet elevation and sea ice interact, which will be discussed below.

3.3. The Impact of AIS–Sea Ice Feedbacks on $\delta^{18}O$, Temperature, and Precipitation

Antarctic sea ice extent increases by 7.6% for the DC -1 km experiment and decreases by 10.8% for the DC $+1$ km experiment (Figure 1). This confirms the AIS feedback on sea ice identified by Singh et al. (2016) (for the case of a 90% flattening of AIS compared to PI). Changes in surface wind stress affect the westerly momentum transfer to the ocean (Schmittner et al., 2011), modulating Northward Ekman transport and the associated Ekman drift of sea ice (Singh et al., 2016). In our simulations, a decrease in AIS elevation results in a noticeable reduction of the easterlies around $72^{\circ}S$ and westerlies around $52^{\circ}S$ (of approximately 8% and 5% , respectively, for DC -1 km), but with little shift in the maximum latitudes of wind speed (Supporting information Figure S2). These changes are likely driven via katabatic–easterlies–westerlies interactions (Sime

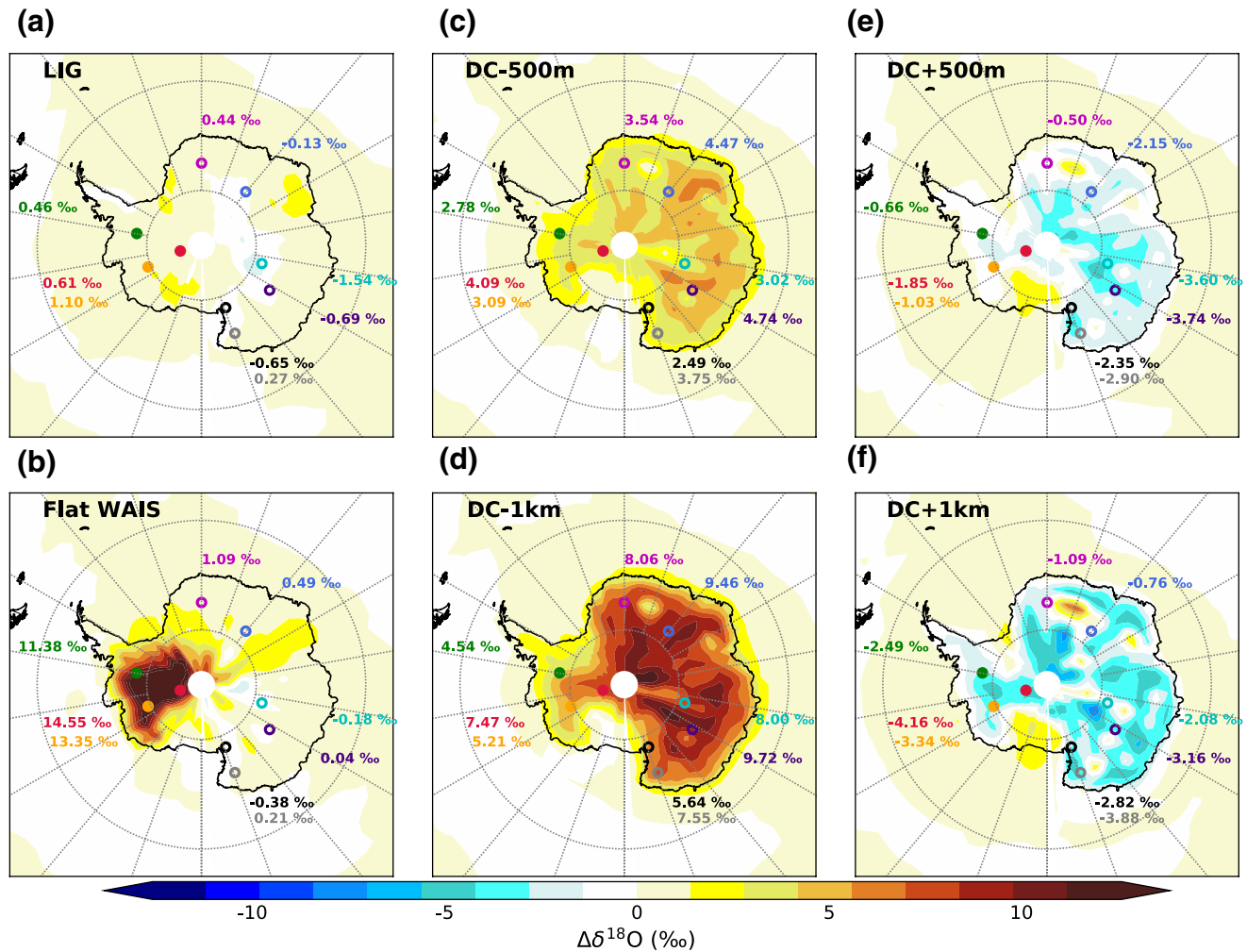


Figure 2. Patterns of $\Delta\delta^{18}\text{O}$ anomalies. Maps of $\Delta\delta^{18}\text{O}$ anomalies against the preindustrial control experiment for (a) the Last Interglacial control experiment, (b) the “Flat WAIS” experiment of Holloway et al. (2016) corresponding to a remnant 200 m West Antarctic Ice Sheet, our Antarctic elevation change in response to elevation scaling of (c) -500 m, (d) -1 km, (e) +500 m, and (f) +1 km, relative to the height at EDC. Points correspond to ice core locations: Vostok (dark green), Dome F (dark blue), EPICA Dome C (gray), EPICA Dronning Maud Land (red), Talos Dome (light green), Taylor Dome (dark violet), Hercules Dome (black), and Skytrain (magenta). Filled points correspond to locations with no available $\delta^{18}\text{O}$ data. EDC, EPICA Dome C.

et al., 2013) and are important to explain the simulated sea ice changes: under DC - 1 km, a smaller volume of sea ice is pushed north, toward warmer waters.

However, it is noteworthy that the sea ice changes can be modified if WAIS and EAIS are adjusted independently; Steig et al. (2015) found a decrease in sea ice extent with a decrease in WAIS elevation. Thus, the sign of sea ice change depends on the details of the topographic change.

Even for our simple linearly scaled AIS scenarios, sea ice changes are spatially nonuniform around Antarctica. Sea ice extent changes are particularly variable with respect to AIS elevation in the Bellingshausen sector: a 50% increase occurs for the DC - 1 km experiment (Supporting information Table S4 and Figure S3). This is likely also related to differing wind forcing, and thus sea ice export, associated with a more stationary and stronger Amundsen Sea low when AIS topography is lower (Krinner & Genthon, 1999; Steig et al., 2015). The Weddell sector shows particularly small changes ($\pm 5\%$). Variability in other sectors remains within a $\pm 15\%$ range. The Bellingshausen and Weddell sectors also stand out in that they present nonlinear AIS-sea ice relationships. Considering the other sectors separately, the mean rate of sea ice area change is -1% per 100 m of elevation change at Dome C (with a mean correlation coefficient of 0.93 and a p -value < 0.05).

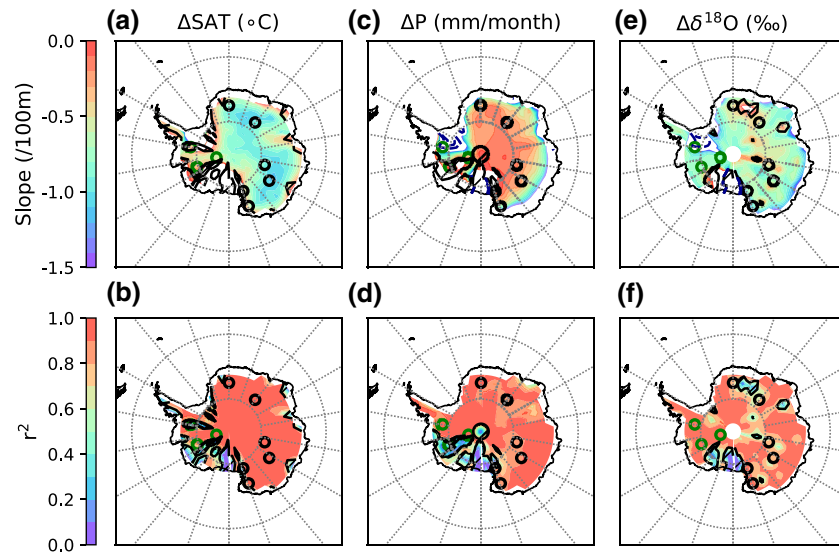


Figure 3. Continental-scale elevation gradients. Slopes (“Slope,” panels (a), (c), and (e)) and variance (“ r^2 ,” panels (b), (d), and (f)) between the deviations of simulated surface air temperature (“ Δ SAT,” slope in $^{\circ}\text{C}/100\text{ m}$), precipitation (“ Δ P,” slope in $\text{mm}/\text{month}/100\text{ m}$), and $\delta^{18}\text{O}$ (“ $\Delta\delta^{18}\text{O}$,” slope in $\text{‰}/100\text{ m}$) compared to the Last Interglacial control simulation, and the elevation at each grid point. In the Weddell region, slopes for precipitation and $\delta^{18}\text{O}$ can be particularly low and are thus shown by blue contours (-20 and $-50^{\circ}\text{C}/100\text{ m}$ for temperature, -20 and $-50\text{ mm}/\text{month}/100\text{ m}$). Nonsignificant relationships are hatched. Ice core locations with available data are indicated by black points, whereas locations with no available data are indicated by green points.

In terms of their control on temperature, precipitation, and $\delta^{18}\text{O}$, these sea ice changes are small compared with the changes in sea ice explored in Holloway et al. (2016). Removing the AIS–sea ice feedbacks on $\delta^{18}\text{O}$ using a linear relationship (Supporting information Figure S4) has a very small effect on precipitation ($-3.0 \pm 1.7\%$ and $4.4 \pm 2.4\%$ changes compared to the LIG control simulation for the DC + 1 km and DC – 1 km simulations, respectively), SAT ($0.4 \pm 0.5\%$ and $-0.5 \pm 0.7\%$ changes compared to the LIG control simulation for the DC + 1 km and DC – 1 km simulations, respectively) and $\delta^{18}\text{O}$ anomalies ($0.9 \pm 0.4\%$ and $-1.4 \pm 0.6\%$ changes compared to the LIG control simulation for the DC + 1 km and DC – 1 km simulations, respectively).

The small size of these indirect AIS–sea ice mediated impacts on temperature, precipitation, and $\delta^{18}\text{O}$ lends confidence to the strategy of treating AIS and sea ice change impacts on $\delta^{18}\text{O}$ as effectively independent of each other (Chadwick et al., 2020; Holloway et al., 2016, 2017). In the following, we thus consider we can quantify the $\delta^{18}\text{O}$ versus elevation relationship independently from other effects.

3.4. Linear SAT–Elevation and $\delta^{18}\text{O}$ –Elevation Relationships

Werner et al. (2018) and Sutter et al. (2020) explored the use of $\delta^{18}\text{O}$ (and SAT) versus elevation relationships to help to evaluate possible AIS reconstructions for the LGM and LIG, respectively. In each case, they used a linear relationship between climate variables and elevation to ascertain past AIS changes. Here, we can use our simulations to assess whether the SAT and $\delta^{18}\text{O}$ versus elevation relationships used in these studies are supported by our suite of LIG simulations. To do this, we calculate slopes for these relationships, using all simulations on a grid point-by-grid point basis (Figures 3 and 4, and Supporting information Text S2).

The Ross Sea, Amundsen Sea, and the coastal regions ($\leq 1,000\text{ m a.s.l.}$) show no significant linear relationships, likely because the intersimulation noise in these quantities is larger than the signal, due to the small elevation changes prescribed in these regions. Outside these regions, where elevation changes are larger, slopes increase from the coast to the plateau. Mean slopes for Δ SAT versus elevation are $-0.34 \pm 0.24^{\circ}\text{C}/100\text{ m}$ for regions currently between 1,000 and 2,000 m a.s.l. This rises considerably to $-0.92 \pm 0.11^{\circ}\text{C}/100\text{ m}$ for regions above 3,000 m a.s.l. (Supporting information Table S5). In both case, these differ from the present-day spatial Δ SAT versus elevation documented by Frezzotti et al. (2007,

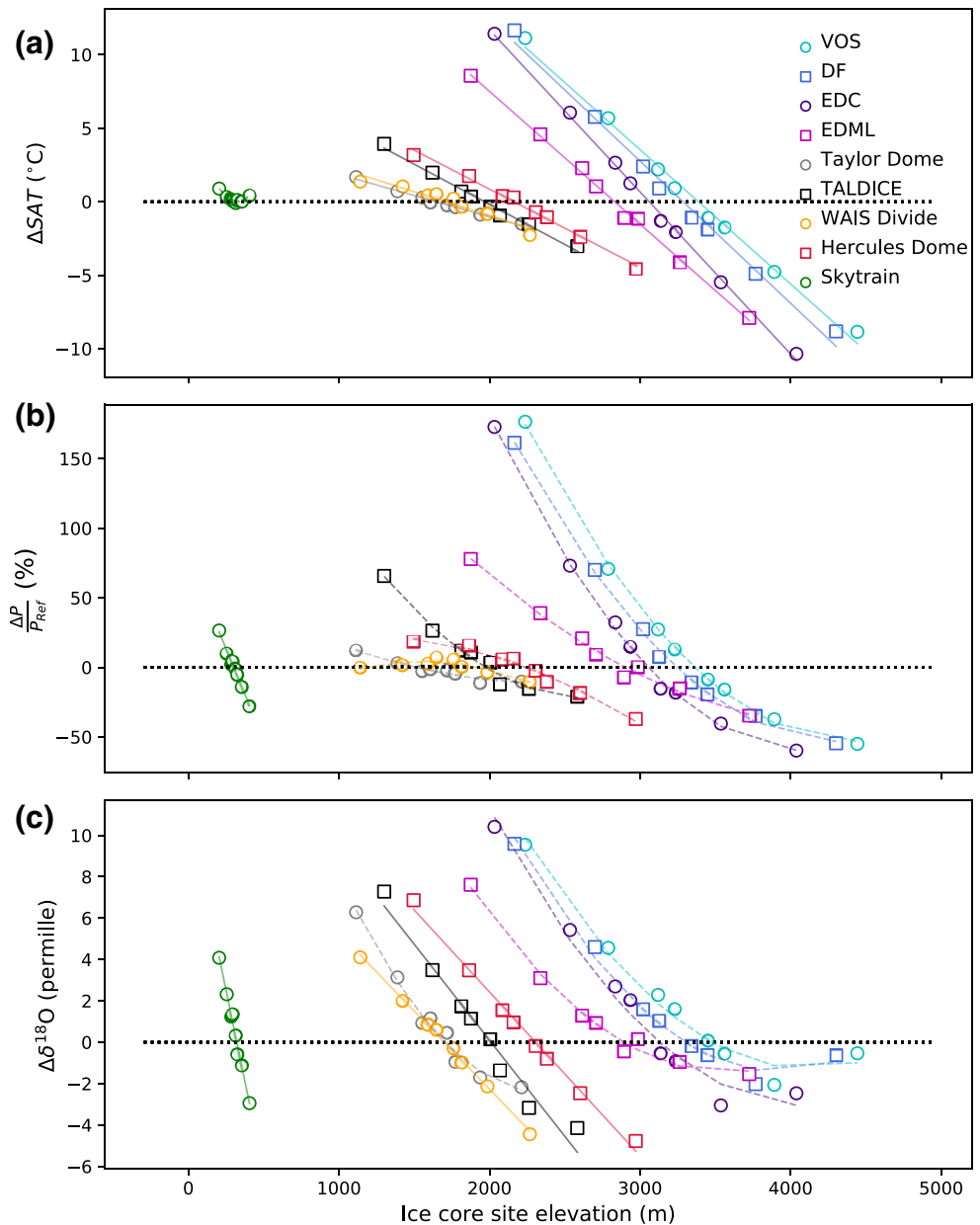


Figure 4. Ice core site elevation gradients. Deviations in ice core (a) surface air temperature (“ ΔSAT ,” in $^{\circ}\text{C}$), (b) precipitation flux (“ $\Delta P/P_{\text{Ref}}$ ” in %), and (c) $\delta^{18}\text{O}$ ($\Delta\delta^{18}\text{O}$, in ‰) compared to the Last Interglacial control simulation, against the site elevation (in m) for a range of Antarctic ice core sites discussed in the text: Vostok (“VOS”), Dome F (“DF”), EPICA Dome C (“EDC”), EPICA Dronning Maud Land (“EDML”), Taylor Dome (“Taylor Dome”), Talos Dome (“TALDICE”), WAIS Divide (“WAIS Divide”), Hercules Dome (“Hercules Dome”), and Skytrain (“Skytrain”). Dots are associated with ice core sites, solid lines emphasize strong linear relationships, and dashed lines strong 2-degree polynomials (i.e., for correlation coefficients higher than 0.9).

$-0.8^{\circ}\text{C}/100\text{ m}$) and Masson-Delmotte et al. (2008, $-1.1^{\circ}\text{C}/100\text{ m}$) (and subsequently used by other authors to calculate past elevation changes). Correlation coefficients for ΔSAT –elevation are higher than 0.9 for all the grid points with significant relationships.

Changes in precipitation (ΔP) and $\Delta\delta^{18}\text{O}$ versus elevation have lower correlation coefficients compared to SAT–elevation relationships, especially on the plateau. Unlike for the SAT–elevation relationships, $\delta^{18}\text{O}$ –elevation slopes are higher in coastal regions compared to the plateau, likely due to source–distance effects on ΔP and, subsequently, $\Delta\delta^{18}\text{O}$ (Figure 3). This feature is also notable at the ice core locations (Figure 4). The

variability of $\Delta\delta^{18}\text{O}$ versus elevation slopes is also spatially larger than for ΔSAT (and ΔP); they vary from $-1.28 \pm 1.38\text{‰}/100\text{ m}$ for regions between 1,000 and 2,000 m a.s.l. to $-0.53 \pm 0.22\text{‰}/100\text{ m}$ for regions above 3,000 m a.s.l. This high variability is also reflected in the $\Delta\delta^{18}\text{O}$ versus elevation calculated at ice core locations (Supporting information Table S6), with the largest slope at the coastal Skytrain location ($-3.52\text{‰}/100$) and smallest slopes on the EAIS plateau, for example, $-0.48\text{‰}/100\text{ m}$ at EDML.

Comparing our simulated relationships to those used by Sutter et al. (2020) to interpret the TALDICE $\delta^{18}\text{O}$ ice core measurements, our simulations would suggest that the relationship used in Sutter et al. (2020) would underestimate the sensitivity of $\Delta\delta^{18}\text{O}$ to elevation change by 43% in this region (Supporting information Text S3): they use a SAT versus elevation slope of $-0.8^\circ\text{C}/100\text{ m}$ (which seems to be an overestimate, see Table S6) multiplied by a $\delta^{18}\text{O}$ versus temperature slope of $0.66\text{‰}/^\circ\text{C}$, to obtain a $\delta^{18}\text{O}$ –elevation relationship of $-0.53\text{‰}/100\text{ m}$, a $\delta^{18}\text{O}$ –elevation relationship of $0.53\text{‰}/100\text{ m}$. These relationships were inferred from present-day values, whereas it might have changed with time. Using our simulations, we thus look at the $\Delta\delta^{18}\text{O}$ versus elevation relationship (LIG temporal relationship) and show that this relationship at this site is $-0.93\text{‰}/100\text{ m}$. For the elevation change they simulate in the case of Wilkes Basin ice collapse, using our LIG temporal relationship, this would lead to an inferred TALDICE $\delta^{18}\text{O}$ increase from 11‰ to 19‰, that is, 73%–83% higher than suggested. This implied underestimation of the inferred $\delta^{18}\text{O}$ from the grounding retreat, reinforces the conclusions of Sutter et al. (2020), emphasizing that TALDICE is an highly sensitive site for indicating EAIS LIG changes, and exclude the Wilkes Basin loss of ice scenarios, since the TALDICE LIG-PI $\delta^{18}\text{O}$ measured change is only 2‰ (Masson-Delmotte et al., 2008).

One of the reasons for the mismatch between our and the Sutter et al. (2020) calculations is their use of a relationship between $\delta^{18}\text{O}$ –temperature not specific to LIG, in the use of calculating past AIS change. Indeed, as for Werner et al. (2018), we find different relationships for different times. If we use all grid points above 100 m a.s.l., a continent-wide average of the slope yields $-0.83 \pm 0.71\text{‰}/100\text{ m}$ ($r = -0.9$). This LIG-PI $\Delta\delta^{18}\text{O}$ –elevation slope is similar to, but slightly higher than the LGM-PI slope obtained by Werner et al. (2018) (slope of $-0.71 \pm 0.3\text{‰}/100\text{ m}$). Similarly to Werner et al. (2018), we thus obtain a continent-wide temporal $\Delta\delta^{18}\text{O}$ –elevation slope, which is 30% lower than the observational present-day spatial $\delta^{18}\text{O}$ –elevation slope (slope of $-1.0\text{‰}/100\text{ m}$, $r = -0.9$, Masson-Delmotte et al., 2008) and the HadCM3 simulated one (slope of $-1.07 \pm 0.02\text{‰}/100\text{ m}$, $r = -0.89$). This, alongside the above, confirms that the use of a present-day spatial elevation gradient as a surrogate for temporal changes for LIG-PI changes must be done with a great deal of care, as it may be incorrect for a variety of locations, AIS changes, and changes through time. Finally we note that, as suggested by Sime et al. (2009), Noone (2009), Figure 4 clearly shows that for a variety of locations, $\Delta\delta^{18}\text{O}$ does not vary in a linear way, so the use of any single gradient, even for a given ice core site, may vary with time and elevation.

4. Conclusions

Overall, we see that elevation-induced changes in $\delta^{18}\text{O}$ follow those in SAT. Larger changes in SAT with elevation occur in coastal regions compared to the plateau. While both $\delta^{18}\text{O}$ and precipitation tend to follow SAT changes when site elevation changes, differences do occur in East Antarctic coastal areas where the orographic slope is high. Compared to the eastern part, the Peninsula and WAIS coastal regions display opposite trends, that is, increasing (decreasing) precipitation with increasing (decreasing) AIS elevation. This suggests the need to (i) employ caution, (ii) model $\delta^{18}\text{O}$, and (iii) drill other ice core species according to accurate WAIS change scenarios to understand how WAIS change will imprint on WAIS ice cores. We note that Antarctic sea ice extent has a relatively modest response to our elevation change experiments. This leads to a small feedback of elevation on climate parameters through sea ice and tends to support the approach that we can look at the controls of sea ice and AIS change on ice core measurements independently (Holloway et al., 2016, 2017).

We find a continental-wide average of the $\Delta\delta^{18}\text{O}$ versus elevation relationship of $-0.83 \pm 0.71\text{‰}/100\text{ m}$ ($r = -0.9 \pm 0.29$), thus 20% lower than the PI spatial slope, confirming that the spatial PI $\delta^{18}\text{O}$ versus elevation relationship cannot be a surrogate for temporal relationships (Werner et al., 2018). We find that relationships vary significantly between different ice core locations, ranging from $-3.52\text{‰}/100\text{ m}$ at Skytrain to $-0.48\text{‰}/100\text{ m}$ at EDML.

Confidently dated ice core measurements covering the LIG are currently only available from East Antarctic ice core sites. Given the widespread expectation of major changes in WAIS elevation during the LIG, there is a need for new well dated ice cores covering the LIG from sites outside the EAIS, alongside further $\delta^{18}\text{O}$ modeling. New ice cores drilled on the WAIS, particularly at Skytrain or Hercules Dome, will provide important insights for future AIS LIG reconstructions. The results above enable ice core $\delta^{18}\text{O}$ measurements to be interpreted from an elevation point-of-view with more certainty.

Finally, we note that this study is limited by the model resolution of HadCM3 and our particular simulation set-up: prescribing small absolute changes in elevation in coastal regions. The Skytrain site would thus benefit from high-resolution modeling, ideally using a regional isotope-enabled climate model.

Data Availability Statement

The orography, surface air temperature, precipitation, and water stable isotope responses to idealized changes in AIS elevation simulated by the isotope-enabled coupled ocean–atmosphere–sea ice General Circulation Model HadCM3 are available on the data system managed by the UK Polar Data Centre (Goursaud et al., 2020) under the Open Government License (<http://www.nationalarchives.gov.uk/doc/open-government-licence/version/3/>).

Acknowledgments

S.G., E.W., and L.S were funding through the European Research Council under the Horizon 2020 research and innovation program (grant agreement no. 742224, WACSWAIN). E.W. is also supported by a Royal Society Professorship. L.S. and M.H. acknowledge support through NE/P013279/1, NE/P009271/1, and EU-TiPES. The project has received funding from the European Union's Horizon 2020 research and innovation program under grant agreement number 820970. This material reflects only the author's views and the Commission is not liable for any use that may be made of the information contained therein.

References

- Adusumilli, S., Fricker, H. A., Medley, B., Padman, L., & Siegfried, M. R. (2020). Interannual variations in meltwater input to the Southern Ocean from Antarctic ice shelves. *Nature Geoscience*, *100*, 616–620.
- Bentley, M. J., Cofaigh, C., Anderson, J. B., Conway, H., Davies, B., Graham, A. G., et al. (2014). A community-based geological reconstruction of Antarctic ice sheet deglaciation since the last glacial maximum. *Quaternary Science Reviews*, *100*, 1–9. <https://doi.org/10.1016/j.quascirev.2014.06.025>
- Chadwick, M., Allen, C., Sime, L., & Hillenbrand, C.-D. (2020). Analysing the timing of peak warming and minimum winter sea-ice extent in the southern ocean during MIS 5e. *Quaternary Science Reviews*, *229*, 106134.
- Conway, H., Hall, B. L., Denton, G. H., Gades, A. M., & Waddington, E. D. (1999). Past and future grounding-line retreat of the West Antarctic ice sheet. *Science*, *286*(5438), 280–283. <https://doi.org/10.1126/science.286.5438.280>
- DeConto, R. M., & Pollard, D. (2016). Contribution of Antarctica to past and future sea-level rise. *Nature*, *531*(7596), 591–597.
- Dutton, A., Carlson, A. E., Long, A. J., Milne, G. A., Clark, P. U., DeConto, R., et al. (2015). Sea-level rise due to polar ice-sheet mass loss during past warm periods. *Science*, *349*(6244), aaa4019. <https://doi.org/10.1126/science.aaa4019>
- Edwards, T. L., Brandon, M. A., Durand, G., Edwards, N. R., Golledge, N. R., Holden, P. B., et al. (2019). Revisiting Antarctic ice loss due to marine ice-cliff instability. *Nature*, *566*(7742), 58–64.
- EPICA Community Members (2006). One-to-one coupling of glacial climate variability in Greenland and Antarctica. *Nature*, *444*(7116), 195–198. <https://doi.org/10.1038/nature05301>
- Frezzotti, M., Urbini, S., Proposito, M., Scarchilli, C., & Gandolfi, S. (2007). Spatial and temporal variability of surface mass balance near Talos Dome, East Antarctica. *Journal of Geophysical Research*, *112*, F02032. <https://doi.org/10.1029/2006JF000638>
- Golledge, N. R., Kowalewski, D. E., Naish, T. R., Levy, R. H., Fogwill, C. J., & Gasson, E. G. W. (2015). The multi-millennial Antarctic commitment to future sea-level rise. *Nature*, *526*(7573), 421–425. <https://doi.org/10.1038/nature15706>
- Goursaud, S., Holloway, M., Sime, L., Wolff, E., Valdes, P., Steig, E., & Pauling, A. (2020). *Global monthly outputs of orography, surface air temperature and water stable isotopes for the last interglacial for idealised Antarctic ice sheet simulations run by the isotope-enabled HadCM3*. <https://www.bas.ac.uk/data/uk-pdc/>: UK Polar Data Centre. <https://doi.org/10.5285/09330d14-7f2d-4c12-ad00-08a9cd1fb214>
- Guarino, M.-V., Sime, L. C., Schröder, D., Malmierca-Vallet, I., Rosenblum, E., Ringer, M., et al. (2020). Sea-ice-free Arctic during the Last Interglacial supports fast future loss. *Nature Climate Change*, *10*, 928–932.
- Holden, P., Edwards, N., Wolff, E. W., Lang, N. J., Singarayer, J., Valdes, P., & Stocker, T. (2010). Interhemispheric coupling, the West Antarctic ice sheet and warm Antarctic interglacials. *Climate of the Past*, *6*(4), 431–443.
- Holloway, M. D., Sime, L. C., Allen, C. S., Hillenbrand, C. D., Bunch, P., Wolff, E., & Valdes, P. J. (2017). The spatial structure of the 128 ka Antarctic sea ice minimum. *Geophysical Research Letters*, *44*, 11129–11139. <https://doi.org/10.1002/2017GL074594>
- Holloway, M. D., Sime, L. C., Singarayer, J. S., Tindall, J. C., Bunch, P., & Valdes, P. J. (2016). Antarctic last interglacial isotope peak in response to sea ice retreat not ice-sheet collapse. *Nature Communications*, *7*, 12293. <https://doi.org/10.1038/ncomms12293>
- Jouzel, J., Masson-Delmotte, V., Cattani, O., Dreyfus, G., Falourd, S., Hoffmann, G., et al. (2007). Orbital and millennial Antarctic climate variability over the past 800,000 years. *Science*, *317*(5839), 793–796. <https://doi.org/10.1126/science.1141038>
- Kageyama, M., Sime, L. C., Sicard, M., Guarino, M. V., de Vernal, A., Schroeder, D., et al. (2020). A multi-model CMIP6 study of Arctic sea ice at 127 ka: Sea ice data compilation and model differences. *Climate of the Past Discussions*, *17*, 37–62. <https://doi.org/10.5194/cp-17-37-2021>
- Kawamura, K., Parrenin, F., Lisiecki, L., Uemura, R., Vimeux, F., Severinghaus, J. P., et al. (2007). Northern Hemisphere forcing of climatic cycles in Antarctica over the past 360,000 years. *Nature*, *448*(7156), 912–916. <https://doi.org/10.1038/nature06015>
- Kopp, R. E., Simons, F. J., Mitrovica, J. X., Maloof, A. C., & Oppenheimer, M. (2009). Probabilistic assessment of sea level during the last interglacial stage. *Nature*, *462*, 863–868. <https://doi.org/10.1038/nature08686>
- Kopp, R. E., Simons, F. J., Mitrovica, J. X., Maloof, A. C., & Oppenheimer, M. (2013). A probabilistic assessment of sea level variations within the last interglacial stage. *Geophysical Journal International*, *193*, 711–716. <https://doi.org/10.1093/gji/ggt029>
- Krinner, G., & Genthon, C. (1999). Altitude dependence of the ice sheet surface climate. *Geophysical Research Letters*, *26*(15), 2227–2230.
- Malmierca-Vallet, I., Sime, L. C., Tindall, J. C., Capron, E., Valdes, P. J., Vinther, B. M., & Holloway, M. D. (2018). Simulating the last interglacial Greenland stable water isotope peak: The role of arctic sea ice changes. *Quaternary Science Reviews*, *198*, 1–14.

- Masson-Delmotte, V., Buiron, D., Ekaykin, A., Frezzotti, M., Gallée, H., Jouzel, J., et al. (2011). A comparison of the present and last interglacial periods in six Antarctic ice cores. *Climate of the Past*, 7(2), 397–423. <https://doi.org/10.5194/cp-7-397-2011>
- Masson-Delmotte, V., Hou, S., Ekaykin, A., Jouzel, J., Aristarain, A., Bernardo, R. T., et al. (2008). A review of Antarctic surface snow isotopic composition: Observations, atmospheric circulation, and isotopic modeling. *Journal of Climate*, 21, 3359–3387. <https://doi.org/10.1175/2007JCLI2139.1>
- McKay, R., Naish, T., Powell, R., Barrett, P., Scherer, R., Talarico, F., et al. (2012). Pleistocene variability of Antarctic ice sheet extent in the Ross embayment. *Quaternary Science Reviews*, 34, 93–112. <https://doi.org/10.1016/j.quascirev.2011.12.012>
- Mechoso, C. R. (1980). The atmospheric circulation around Antarctica: Linear stability and finite-amplitude interactions with migrating cyclones. *Journal of the Atmospheric Sciences*, 37(10), 2209–2233.
- Mechoso, C. R. (1981). Topographic influences on the general circulation of the southern hemisphere: A numerical experiment. *Monthly Weather Review*, 109(10), 2131–2139.
- Medley, B., & Thomas, E. (2019). Increased snowfall over the Antarctic ice sheet mitigated twentieth-century sea-level rise. *Nature Climate Change*, 9(1), 34–39.
- Noone, D. (2009). Kink in the thermometer. *Nature*, 462(7271), 295–296.
- Otto-Bliesner, B., Braconnot, P., Harrison, S., Lunt, D., Abe-Ouchi, A., Albani, S., et al. (2017). The PMP4 contribution to CMIP6—Part 2: Two interglacials, scientific objective and experimental design for Holocene and last interglacial simulations. *Geoscientific Model Development*, 10(11), 3979–4003. <https://doi.org/10.5194/gmd-10-3979-2017>
- Otto-Bliesner, B., Brady, E., Zhao, A., Brierley, C., Axford, Y., Capron, E., et al. (2020). Large-scale features of Last Interglacial climate: Results from evaluating the *lig127k* simulations for CMIP6-PMP4. *Climate of the Past Discussions*.
- Parish, T. R., Bromwich, D. H., & Tzeng, R.-Y. (1994). On the role of the Antarctic continent in forcing large-scale circulations in the high southern latitudes. *Journal of the Atmospheric Sciences*, 51(24), 3566–3579.
- Petit, J. R., Raynaud, D., Basile, I., Chappellaz, J., Davisk, M., Ritz, C., et al. (1999). Climate and atmospheric history of the past 420,000 years from the Vostok ice core, Antarctica. *Nature*, 399, 429–436.
- Pollard, D., & DeConto, R. M. (2009). Modelling West Antarctic ice sheet growth and collapse through the past five million years. *Nature*, 458(7236), 329–332. <https://doi.org/10.1038/nature07809>
- Ritz, C., Rommelaere, V., & Dumas, C. (2001). Modeling the evolution of Antarctic ice sheet over the last 420,000 years' implications for altitude changes in the Vostok region. *Journal of Geophysical Research*, 106(D23), 943–974. <https://doi.org/10.1029/2001JD900232>
- Scambos, T., Bell, R., Alley, R., Anandakrishnan, S., Bromwich, D., Brunt, K., et al. (2017). How much, how fast?: A science review and outlook for research on the instability of Antarctica's thwaites glacier in the 21st century. *Global and Planetary Change*, 153, 16–34. <https://doi.org/10.1016/j.gloplacha.2017.04.008>
- Scherer, R. P., Aldahan, A., Tulaczyk, S., Possnert, G., Engelhardt, H., & Kamb, B. (1998). Pleistocene collapse of the West Antarctic ice sheet. *Science*, 281(5373), 82–85. <https://doi.org/10.1126/science.281.5373.82>
- Schmittner, A., Silva, T. A., Fraedrich, K., Kirk, E., & Lunkeit, F. (2011). Effects of mountains and ice sheets on global ocean circulation. *Journal of Climate*, 24(11), 2814–2829.
- Sime, L. C., Carlson, A., & Holloway, M. (2019). On recovering last interglacial changes in the Antarctic ice sheet. *Past Global Changes Magazine*, 27(1), 14–15.
- Sime, L. C., Kohfeld, K. E., Le Quéré, C., Wolff, E. W., de Boer, A. M., Graham, R. M., & Bopp, L. (2013). Southern hemisphere westerly wind changes during the last glacial maximum: Model-data comparison. *Quaternary Science Reviews*, 64, 104–120.
- Sime, L. C., Wolff, E. W., Oliver, K. I. C., & Tindall, J. C. (2009). Evidence for warmer interglacials in East Antarctic ice cores. *Nature*, 462, 342–345. <https://doi.org/10.1038/nature08564>
- Singh, H. K., Bitz, C. M., & Frierson, D. M. (2016). The global climate response to lowering surface orography of Antarctica and the importance of atmosphere–ocean coupling. *Journal of Climate*, 29(11), 4137–4153.
- Steig, E. J., Ding, Q., White, J. W., Küttel, M., Rupper, S. B., Neumann, T. A., et al. (2013). Recent climate and ice-sheet changes in west Antarctica compared with the past 2,000 years. *Nature Geoscience*, 6(5), 372–375.
- Steig, E. J., Huybers, K., Singh, H. A., Steiger, N. J., Ding, Q., Frierson, D. M., et al. (2015). Influence of West Antarctic Ice Sheet collapse on Antarctic surface climate. *Geophysical Research Letters*, 42, 4862–4868. <https://doi.org/10.1002/2015GL063861>
- Steig, E. J., Morse, D. L., Waddington, E. D., Stuiver, M., Grootes, P. M., Mayewski, P. A., et al. (2000). Wisconsinan and Holocene climate history from an ice core at Taylor Dome, Western Ross Embayment, Antarctica. *Geografiska Annaler - Series A: Physical Geography*, 82(2–3), 213–235.
- Stenni, B., Buiron, D., Frezzotti, M., Albani, S., Barbante, C., Bard, E., et al. (2011). Expression of the bipolar see-saw in Antarctic climate records during the last deglaciation. *Nature Geoscience*, 4(1), 46–49. <https://doi.org/10.1038/ngeo1026>
- Sutter, J., Eisen, O., Werner, M., Grosfeld, K., Kleiner, T., & Fischer, H. (2020). Limited retreat of the Wilkes Basin ice sheet during the last interglacial. *Geophysical Research Letters*, 47, e2020GL088131. <https://doi.org/10.1029/2020GL088131>
- Sutter, J., Gierz, P., Grosfeld, K., Thoma, M., & Lohmann, G. (2016). Ocean temperature thresholds for last interglacial West Antarctic ice sheet collapse. *Geophysical Research Letters*, 43, 2675–2682. <https://doi.org/10.1002/2016GL067818>
- Tindall, J. C., Valdes, P. J., & Sime, L. C. (2009). Stable water isotopes in HadCM3: Isotopic signature of El Niño–Southern Oscillation and the tropical amount effect. *Journal of Geophysical Research*, 114, D04111. <https://doi.org/10.1029/2008JD010825>
- Werner, M., Jouzel, J., Masson-Delmotte, V., & Lohmann, G. (2018). Reconciling glacial Antarctic water stable isotopes with ice sheet topography and the isotopic paleothermometer. *Nature Communications*, 9(3537). <https://doi.org/10.1038/s41467-018-05430-y>
- Wilson, D. J., Bertram, R. A., Needham, E. F., van de Flierdt, T., Welsh, K. J., McKay, R. M., et al. (2018). Ice loss from the East Antarctic ice sheet during late Pleistocene interglacials. *Nature*, 561(561), 383–386. <https://doi.org/10.1038/s41586-018-0501-8>